気象研究所研究報告　第45巻第2号　51-63頁　平成6年12月
Papers in Meteorology and Geophysics　Vol. 45, No. 2, pp.51-63, December 1994

Numerical Simulation of Regional Scale Dispersion of Radioactive Pollutants from the Accident at the Chernobyl Nuclear Power Plant

by

Takehiko Satomura, Fujio Kimura*, Hidetaka Sasaki,

Tomoaki Yoshikawa

Meteorological Research Institute, Tsukuba, Ibaraki, 305 Japan

and

Yoshitaka Muraji**

International Meteorological Oceanographic Consultant, Shintomi, Chuou-ku, Tokyo, 104 Japan

(Received March 31, 1994 ; Revised November 15, 1994)

Abstract

Air concentration and deposition of radioactive pollutants in Europe after the Chernobyl nuclear power plant accident is simulated using a long-range transport model developed in the MRI. This model is composed of the weather forecasting part which was the routine regional weather forecasting model of the JMA and the Lagrangian advection-diffusion part. The source data distributed by the ATMES project is used to determine the initial release rate from the power plant.

Calculated concentrations of Cs-137 and I-131 in the surface level atmosphere agree well with observation. Surface deposition of Cs-137 has, however, poor correlation with the observed deposition. Bad precipitation forecast of the weather forecasting part of the model and the difference between the horizontal scale represented by observation and by simulation are considered to be responsible for this poor correlation.

*) Present affiliation : Institute of Geoscience, Univ. of Tsukuba, Tsukuba, Ibaraki, 305 Japan
**) Present affiliation : Energy Sharing Co., Ltd., Arakawaoki-Nishi, Tsuchiura, 300-11 Japan

1. Introduction

Recently, regional and international concern on air pollution has increased, and with it needs for tools to evaluate long-range transport of pollutants have augmented. In the Meteorological Research Institute, a Lagrangian air pollution transport model has been developed to simulate air pollutants related with acid rain over Eastern Asia. Although databases of released and concentrated pollutants averaged over the time scales of months are well established (for example, Johnson, 1983; Air and Energy Engineering Research Lab., 1989), observation of air concentration and deposition of pollutants released from a well-defined source is hardly available; this kind of data is indispensable to evaluate and improve the long-range transport model.

On April 25, 1986, a serious accident occurred at the Chernobyl nuclear power plant, USSR, and a large amount of radioactive substances were released into the atmosphere. Because of its serious impact over Europe, studies of the movement and deposition of radioactive substances have been completed (for example, Kimura and Yoshikawa, 1988; Hass *et al.*, 1990; Puhakka *et al.*, 1990). These studies have established the following: the radioactive clouds released by the main explosion of the plant was transported northward very fast in the warm conveyor belt and deposited over northern Europe in the first several days after the explosion. On 30 April, the radioactive cloud marched to central Europe. At the same time, a part of the pollutants transported to the middle troposphere moved eastward at high speed and reached Japan on 4 May 1986.

Deposited radioactive pollutants have serious effects on lives on the surface and, therefore, they should also be analyzed and predicted precisely. In the case of Chernobyl, wet deposition is believed to be important in the northern and central European areas (Hass *et al.*, 1990; Puhakka *et al.*, 1990). In the United Kingdom, Clark and Smith (1988) investigated distribution of dry and wet deposition of I-131 and Cs-137 after the accident. The amount of deposited Cs-137 correlated well with precipitation. This means that the wet deposition seems to be dominant for Cs-137. On the other hand, distribution of deposited I-131 was quite different from that of Cs-137, so that the dry deposition can be expected to be more important for I-131. On the global scale, Pudykiewicz (1990) reported the distribution of the radioactive pollutant simulated by a global scale predictive tracer model. He calculated the pollutant distribution by both diagnostic mode and fully predictive mode of the model and compared the results with the observation. The model includes dry and wet deposition, but the amount of deposited radioactivity was not compared with observation.

The mechanism of transport and removal of the radioactive pollutant would be similar to that of the long-range transport of sulphate and nitrate, which are the main precursors of acid rain. The accident gave us a chance to evaluate the accuracy of the long-range transport model for acid rain such as the model used here.

In this study, the MRI long-range transport model is evaluated in the case of the Chernobyl accident. The emission and observational data on air and deposited concentration of radioactive pollutants used in this study were the data distributed in a project named ATMES (Joint IAEA / WMO / CEC Atmospheric Transport Model Evaluation Study). This project was started a few months after the accident, and the aim of the project was to review and intercalibrate atmospheric transport models using the observational data of the Chernobyl accident (Klug, *et al.*, 1991a). In this project, a time series of the released amount of radioactive pollutants with their effective heights and time series of surface air concentration and of deposited amounts of radioactive pollutants observed over Europe were distributed. Though the amount and the form of the emitted substances are not precisely determined (Petrov, private communication) and up to 3 hours ambiguity remains in the observation time (Raes *et al.*, 1989, 1990), these distributed data are believed to be the best data set over Europe on the Chernobyl accident.

2. Numerical Model

The model consists of two parts: a weather forecasting part which predicts meteorological variables, and an advection-diffusion part of pollutants which uses meteorological variables forecasted by the first part as input data.

2.1. Weather Forecasting Part

This part of the model is almost the same as the old version of the routine weather forecasting model of the Japan Meteorological Agency (JMA). Details of this model are described in a technical report issued by the Numerical Prediction Division of JMA (1986). We modified the topography and physical parameterization in the original forecasting model to apply it to the Chernobyl accident. In this section, a brief description of the model is given for readers' convenience.

2.1.1. Governing Equations

We use the primitive equations in σ-coordinates and the polar stereographic projection at 60°N. The equations are:

$$\frac{\partial}{\partial t}\left(\frac{\pi}{m^2}u\right)+\frac{\partial}{\partial x}(u^*u)+\frac{\partial}{\partial y}(v^*u)+\frac{\partial}{\partial\sigma}\left(\frac{\pi\dot{\sigma}}{m^2}u\right)+\frac{\pi}{m^2}\nu \tag{1}$$
$$\left(f-\nu\frac{\partial m}{\partial x}+u\frac{\partial m}{\partial y}\right)=-\frac{\pi}{m}\frac{\partial\phi}{\partial x}-c_p\frac{\pi\theta}{m}\frac{\partial \mathrm{P}^\kappa}{\partial x}+\mathrm{F}_u-\frac{g}{m^2}\left(\frac{\partial\tau}{\partial\sigma}\right)_x$$

$$\frac{\partial}{\partial t}\left(\frac{\pi}{m^2}\nu\right)+\frac{\partial}{\partial x}(u^*\nu)+\frac{\partial}{\partial y}(v^*\nu)+\frac{\partial}{\partial\sigma}\left(\frac{\pi\dot{\sigma}}{m^2}\nu\right)-\frac{\pi}{m^2}u \tag{2}$$
$$\left(f-\nu\frac{\partial m}{\partial x}+u\frac{\partial m}{\partial y}\right)=-\frac{\pi}{m}\frac{\partial\phi}{\partial x}-c_p\frac{\pi\theta}{m}\frac{\partial \mathrm{P}^\kappa}{\partial x}+\mathrm{F}_v-\frac{g}{m^2}\left(\frac{\partial\tau}{\partial\sigma}\right)_y$$

$$\frac{\partial}{\partial t}\left(\frac{\pi}{m^2}\theta\right)+\frac{\partial}{\partial x}(u^*\theta)+\frac{\partial}{\partial y}(v^*\theta)+\frac{\partial}{\partial\sigma}\left(\frac{\pi\dot{\sigma}}{m^2}\theta\right)$$
$$=\mathrm{F}_\theta+\frac{\pi}{m^2}Q-\frac{g}{c_p m^2 \mathrm{P}^\kappa}\frac{\partial \mathrm{H}}{\partial\sigma} \tag{3}$$

$$\frac{\partial}{\partial t}\left(\frac{\pi}{m^2}q\right)+\frac{\partial}{\partial x}(u^*q)+\frac{\partial}{\partial y}(v^*q)+\frac{\partial}{\partial\sigma}\left(\frac{\pi\dot{\sigma}}{m^2}q\right)$$
$$=\mathrm{F}_q+\frac{\pi}{m^2}\mathrm{M}+\frac{g}{m^2}\frac{\partial \mathrm{E}}{\partial\sigma} \tag{4}$$

$$\frac{\partial}{\partial t}\left(\frac{\pi}{m^2}\right)+\frac{\partial u^*}{\partial x}+\frac{\partial v^*}{\partial y}+\frac{\partial}{\partial\sigma}\left(\frac{\pi\dot{\sigma}}{m^2}\right)=0\ , \tag{5}$$

$$\frac{\partial\phi}{\partial\sigma}=-c_p\theta\frac{\partial \mathrm{P}^k}{\partial\sigma}, \tag{6}$$

where the symbols are as follows

$$m=\frac{1+\sin 60^\circ}{1+\sin\varphi}\ ,$$

φ is the latitude,

$\pi=p_T-p_S$,

p_T : pressure at the model top,

p_S : surface pressure,

$\mathrm{P}=p/p_0$,

u^* and v^* : $\pi u/m$ and $\pi v/m$, respectively,

q : water vapor mixing ratio,

E : vertical eddy flux of water vapor,

H : vertical eddy flux of sensible heat,

M : amount of decrease in water vapor by condensation or precipitation,

τ : Reynolds stress by vertical wind shear,

F_u, F_v, F_θ, F_q : horizontal eddy diffusion of u, v, θ, and q, respectively,

and the other symbols are conventional.

2.1.2. Grid Systems and Difference Schemes

The calculation domain and the topography in the model are shown in Fig. 1. The domain is covered horizontally by Arakawa's B grid (73×55). The grid size d is 127 km at 60°N. The domain is divided into 16 layers in the vertical direction as shown in Fig. 2. Finite difference schemes in space are based on Arakawa and Lamb (1977), and time difference scheme is Tatsumi's "economical explicit scheme" (Tatsumi, 1983).

2.1.3. Boundary Conditions

At the upper and the lower boundaries, we assume $\dot{\sigma}=0$. At the lateral boundaries, we apply the Hovermale condition by adding the following term to the right-hand sides of eqs. (1)−(5):

$$\mathrm{K}\left(\frac{l}{L}\right)^\beta\nabla_X^2(A-A_B), \tag{8}$$

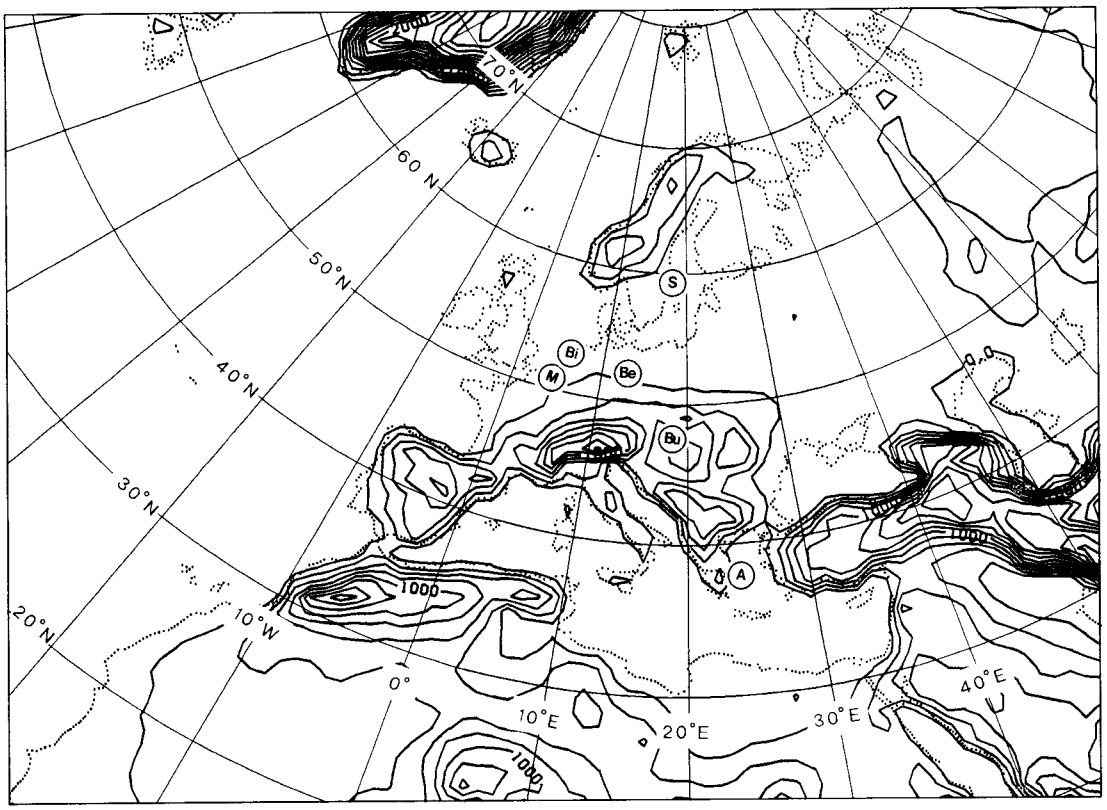

Fig.1. Domain of integration. Coast lines are indicated by dots. Contour for terrain elevation (solid line) begins at 200 m, at intervals of 200 m. Points labeled "S", "Bu", "M", "A", "Bi" and "Be" are Stockholm, Budapest, Mol, Attikis, Bilthoven and Berlin, respectively.

where A is a physical variable, A_B is a prescribed boundary value, l is the distance from the boundary,

$K=4\times10^{-4}\mathrm{sec}^{-1}$,
$L=6d$,
$\beta=1.5$,

and,

$$\nabla_{\times}^{2}A_{(x,y)}\equiv A_{(x-d,y+d)}+A_{(x+d,y-d)}+A_{(x-d,y+d)}+A_{(x-d,y-d)}-4A_{(x,y)}, \quad (9)$$

2.1.4. *Parameterization of Physical Processes*

a) Horizontal and vertical diffusion

As the vertical eddy diffusion, we employ the closure model of level 2 (Mellor and Yamada, 1974). At the lowest layer, Monin-Obukov's similarity theory is applied to determine vertical fluxes from the lower boundary. The surface temperature is predicted. As the horizontal eddy diffusion, an artificial 4th order diffusion is applied as follows:

$$F_a \equiv -K_h\nabla\{\pi\nabla(\nabla_{+}^{2}a)\}-K_{div}\pi\nabla\{\nabla_{+}^{2}(\nabla a)\},$$
$$F_b \equiv -K_h\nabla\{\pi\nabla(\nabla_{+}^{2}b)\}, \quad (10)$$

where a is horizontal velocity u or v, b is scalar variable θ or q,

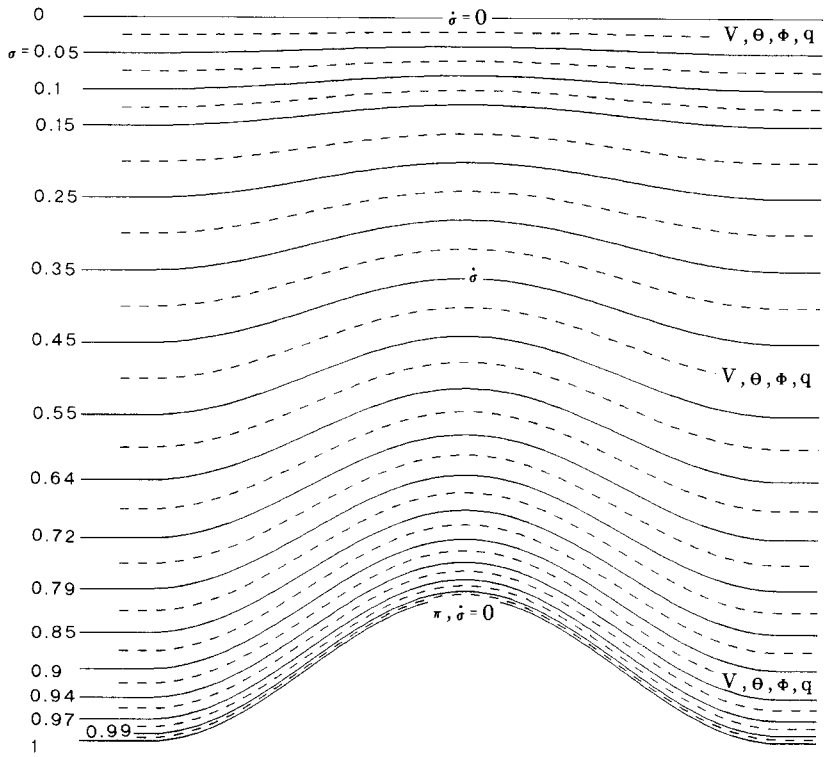

Fig.2. Vertical grid system in σ-coordinate.

$$\nabla^2_{+}A_{(x,y)} \equiv A_{(x+d,y)} + A_{(x-d,y)} + A_{(x,y+d)} + A_{(x,y-d)} - 4A_{(x,y)},$$

$K_h = 5 \times 10^4 m^2/sec,$

$K_{div} = 10 \times 10^4 m^2/sec.$

These terms are introduced to dissipate noise with a very short wavelength, and have no physical meaning.

b) Convection and Condensation

We use two types of parameterization for precipitation process in the model: the large-scale condensation parameterization and the moist convective adjustment. The former prevents supersaturation and the latter keeps the atmospheric lapse rate between the dry adiabatic and the moist adiabatic lapse rate.

2.1.5. Input Data

At the time of the Chernobyl event, a global objective analysis was executed every 12 hours by the JMA. It has 2.5 degrees resolution both in latitude and longitude on 16 pressure levels. From this objective analysis, we prepare initial and boundary data for our model by interpolation.

Sea surface temperature is interpolated from global climatological data with 1 degree resolution in latitude and longitude prepared by Alexander and Mobley (1976).

2.2. Advection-Diffusion Part

Advection and diffusion of radioactive pollutants are described by a random-walk model in the same coordinate systems as in the weather forecasting part. Winds, precipitation and diffusion coefficients used in the random walk model are predicted by the weather forecasting model. The variables are stored at

every one hour integration of the forecast model, but the data of the first 12 hours are not used because the so-called spin-up time of the forecast model is about 12 hours. Therefore, we integrate 36 hours in the forecasting part to create input data for 24 hours integration of the advection-diffusion part.

2.2.1. Governing Equations

The equations of the random walk model are:

$$\begin{cases} \dfrac{dX}{dt} = u, \\ \dfrac{dY}{dt} = v, \\ \dfrac{d\sigma}{dt} = \dot{\sigma} + R, \end{cases} \tag{11}$$

where X, Y, and σ are positions of a particle in the three-dimensional space. A random variable R is defined as

$$R = \pm\sqrt{\frac{2\mathrm{Kz}}{\delta t}}, \tag{12}$$

where Kz is the vertical diffusion coefficient derived from the forecast model, δt is the time interval in the random walk model, and the sign of the right-hand side is chosen randomly for each particle and each time step.

The effect of horizontal subgrid-scale diffusion is not included. The initial plume is broadened by the horizontal and the vertical wind shear.

2.2.2. Time Difference Scheme

A simplified Runge-Kutta method is employed for time integration of three-dimensional advection terms with a long time step $\delta t = 10$ min. We employ the Euler-backward scheme for random vertical diffusion terms with shorter time step $\delta\tau = 2$ min in order to avoid artificial convergence or divergence of particles at the layer where Kz varies abruptly.

2.2.3. Parameterization for Deposition

a) Dry deposition

A particle is assumed to be deposited by a dry process if the following two conditions are satisfied: the height of the particle is lower than a prescribed critical height $h_c = 0.99$ in σ-coordinate, and a number given randomly for each particle and each time step is smaller than a value P_{ddep} defined as

$$P_{ddep} = \frac{V_{dep}\,\delta t}{H_{dep}} \tag{13}$$

where V_{dep} is the dry deposition velocity $H_{dep} = 100$m. In this study, $V_{dep} = 1\times10^{-3}$ m/s is used for I-131. Based on the measurement in the United Kingdom, Clark and Smith (1988) estimated $V_{dep} = 3\times10^{-3}$m/s for I-131. They also showed, however, that the values of deposition velocities were widely distributed. Therefore, $V_{dep} = 1\times10^{-3}$ m/s for I-131 used in this study is not an artificially small value while this value is three times smaller than that they estimated. For Cs-137, $V_{dep} = 5\times10^{-4}$ m/s is used and is the same as the estimate by Clark and Smith (1988).

b) Wet deposition

Wet deposition of the pollutants was estimated every one hour. The particles are deposited on the surface with a probability defined by

$$P_{Wdep} = C_{dep}\cdot\delta t\cdot \mathrm{RR},$$

where C_{dep} is the wet deposition rate, δt the estimated duration of wet deposition (one hour) and RR is a precipitation factor.

The deposition rates for pollutants are difficult to estimate, since they may vary with the phase of the material and meteorological conditions. For SO_2 and SO_4^{-2}, wet deposition rates are estimated to be in the range of $3 \sim 50\times10^{-5}$ s^{-1} and $0.5 \sim 2\times10^{-5}$ s^{-1} (Eliassen, 1980). Pudykiewicz (1990) assumed $C_{dep} = 3.5\times10^{-5}$s^{-1} for Chernobyl radioactive pollutants. In this study, 5×10^{-5}s^{-1} is assumed for the wet deposition rate of I-131 and Cs-137.

The precipitation factor RR is defined as:

- for particles at grid points
  RR = 1 if the predicted precipitation rate is greater than 0.05 mm/hour,
  RR = 0 otherwise,
- for particles between grid points
  RR is interpolated horizontally using RRs

around the particle.

2.2.4. Source Terms

a) Release height

The release heights described in the ATMES technical specification document included in Klug *et al.* (1991b) are converted to σ level as:

300m ——— σ=0.965
600m ——— σ=0.954
1500m ——— σ=0.853

b) Other source term characteristics

We assume the normal distribution in both horizontal and vertical directions. The standard deviation used in this model is 127km/2=63.5km in the horizontal direction and 0.05 in the σ level (vertical direction).

Release rates of radioactive aerosol, specified in the ATMES Protocols, are shown in Fig. 3. As a correction of disintegration, 8.02 days is used for a half-life day of I-131.

2.2.5. Concentration calculation

The number of released particles is 20000 in each for the cases of I-131 and for Cs-137. To obtain the surface air concentration at a location, particles within a box of 2 horizontal grid lengths (~250 km) from the location and 0.1 vertical length in σ coordinate (~1 km) are counted and the number of particles is converted into the concentration. To obtain the deposited concentration at a location, the particles within an area of 2 horizontal grid lengths from the location are counted and converted into the amount of deposition.

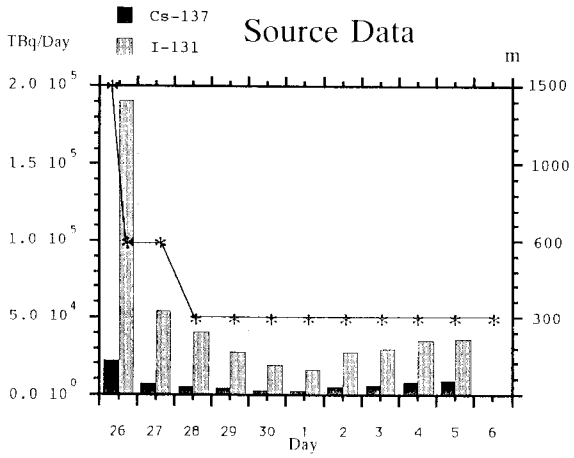

Fig.3. Time change of Cs-137 (black bar) and I-131(grey bar) release (unit in Terra Bq/day) by the Chernobyl accident. Solid line with asterisk is the effective initial plume center of mass height (unit in meters).

3. Results

3.1. Movement of pollutants

Figure 4 shows forecasted weather maps and radioactive clouds. The model predicts the weather pattern well, compared with the objective analysis of the JMA: centers of cyclones and anticyclones are predicted with errors less than about 500 km and 4~8 hPa except two cases. The two exceptional cases are over the Adriatic Sea on April 29, where the model predicts a too strong cyclone, and over south England on May 3, where the model predicts a too weak cyclone (not shown). Although the strong (weak) cyclone over the Adriatic Sea (south England) may attract the radioactive cloud stronger (weaker) than the observation, the model is expected to represent the overall movement of the radioactive cloud in good accuracy.

The radioactive cloud released at Chernobyl on April 26 moved northwestward and reached the Swedish coast of the Baltic sea in only two days. Thus, the speed of the pollutants averaged in these first two days is about 10 m/sec. This rapid movement indicates that a warm conveyor belt formed by a low pressure zone over western

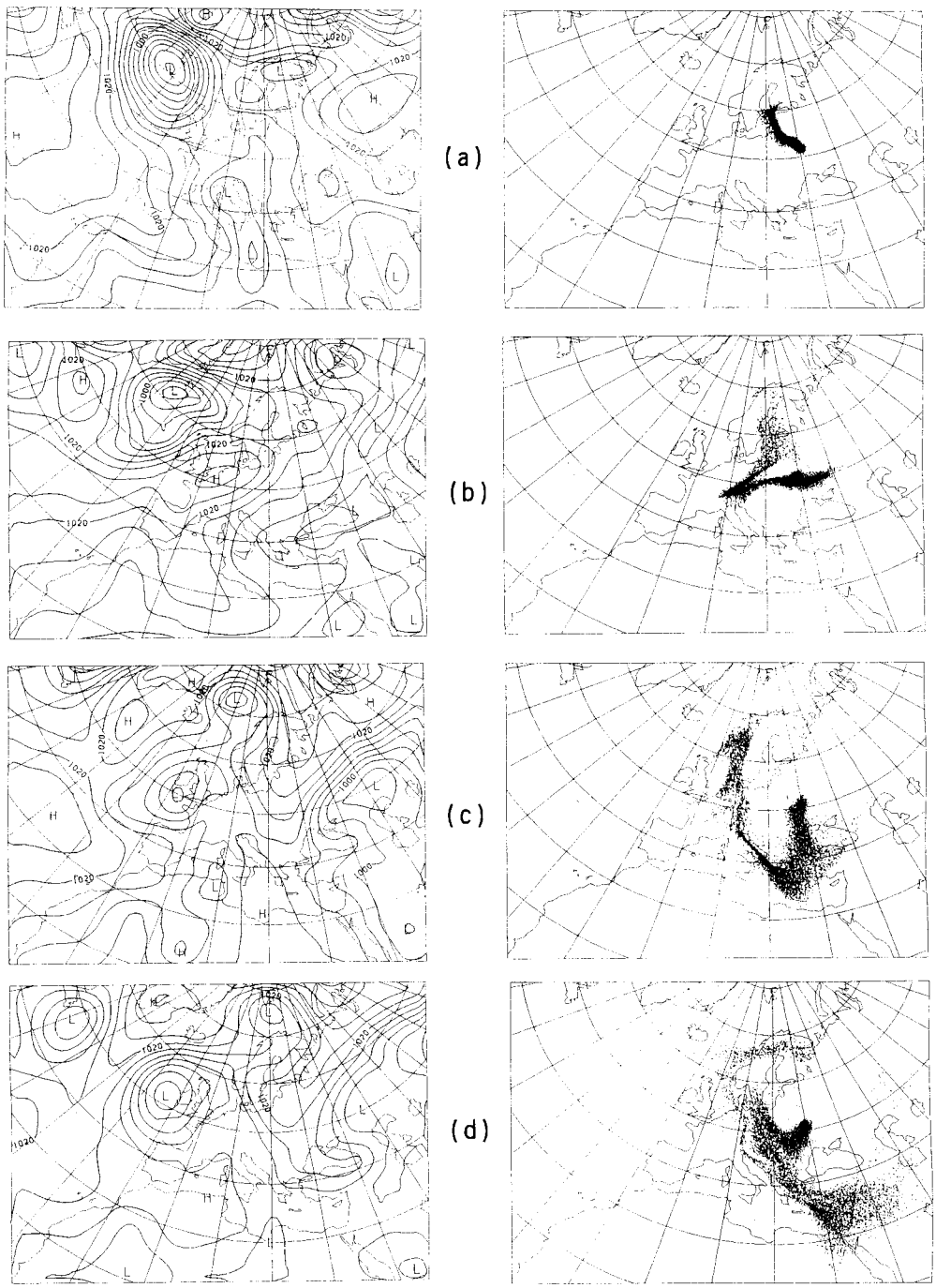

Fig.4. Forecasted surface pressure map (left column) and position of Cs-137 particles in the air (right column) at 00 UTC (a) 28 April ; (b) 1 May ; (c) 4 May ; (d) 6 May. Contour interval of surface pressure is 4 hPa.

Europe and the north Atlantic Ocean transported the pollutants. This movement coincides with the trajectory analysis by Puhakka *et al.* (1990).

After April 30, the pollutants released early on entered the cold section of the cyclone over southern Europe and they were transported southwestward by a cold conveyor belt to Austria and Swiss. On the other hand the pollutants released later moved in the southerly direction and reached over Greek, Turkey and the Mid-East countries.

Pollutants released after May 5 migrated over Eastern Europe in a few days and gradually moved further to the East.

3.2. Comparison with surface observations of air concentration

Observed data of radioactive pollutants at about ninety stations for air concentration and about thirty for deposition were distributed by the ATMES steering committee (Raes *et al.*, 1989) and stored in the data bank named REM Data Bank (Raes *et al.*, 1990). We selected four stations Stockholm, Mol, Budapest and Attikis from the distributed list of observation stations and compared observed pollutants with calculated values. We chose the points because the locations of these four stations ranges over the whole European Continent (Fig. 1) and they are expected to be typical in the area over which dense pollutant cloud flowed. Figure 5 shows observed and calculated surface air concentration of Cs-137 at Stockholm, Mol, Budapest and Attikis. This figure shows a good correlation between simulated concentration and observation : initial arrival day of pollutants (except at Budapest) and the tendency to increase or decrease in time at each location agrees with observation. Looking into the detail, however, we notice some discrepancies between observation and the model results, especially underestimation of simulated concentration on May 2−4 at Stockholm and after May 7 at Mol. We also notice the delay of the initial arrival time in the simulation at Budapest as mentioned above.

The surface air concentration of I-131 is shown in Fig. 6. Observed concentration patterns are almost the same as in Fig. 5, while the concentration of I-131 was denser than that of Cs-137 (note that the maximum value of the ordinate in Fig. 6 is one order larger than that in Fig. 5). Our model simulates the air concentration of I-131 with almost the same accuracy as that of Cs-137, and the discrepancies mentioned above still exist.

The effect of vertical subgrid-scale diffusion is included in the model by employing a random-walk method as eq. (12). The effect of horizontal subgrid-scale diffusion is, however, not included in the diffusion part nor in the weather forecasting part. The initial plume is broadened only by the horizontal and the vertical wind shear. The pollutant cloud is, therefore, much narrower than the other investigations (for example, Puhakka *et al.*, 1990, and Hass *et al.*, 1990). We suspected that the discrepancy of the air concentration between the model and the observation mentioned above resulted from this lack of horizontal diffusion. Some additional simulations were, therefore, performed to study the effects of subgrid-scale horizontal diffusion. Because no reliable parameterization scheme for models using $\delta x \sim 100$ km is known, we used constant horizontal diffusion coefficients of 2×10^5, 5×10^5, 1×10^6, 2×10^6 m^2/sec. However the results did not indicate clear improvement : the results were improved at some points but had no effect at other points (not shown). Probably, more sophisticated parameterization for the subgrid-scale horizontal diffusion is required to improve the model performance. A long-range transport experiment performed after careful preparation will be great help for choosing the scheme of the horizontal subgrid-scale diffusion.

Two other factors also affect the horizontal width of the pollutant cloud : the initial horizontal and vertical width of the source and the number of released particles. If the initial width is broadened or if the number of particles is increased, the simulated pollutant plume would be broadend. This broadening has a potential to dissolve some part of the above discrepancies in general. In this paper, however, the effects of variation of these parameters are

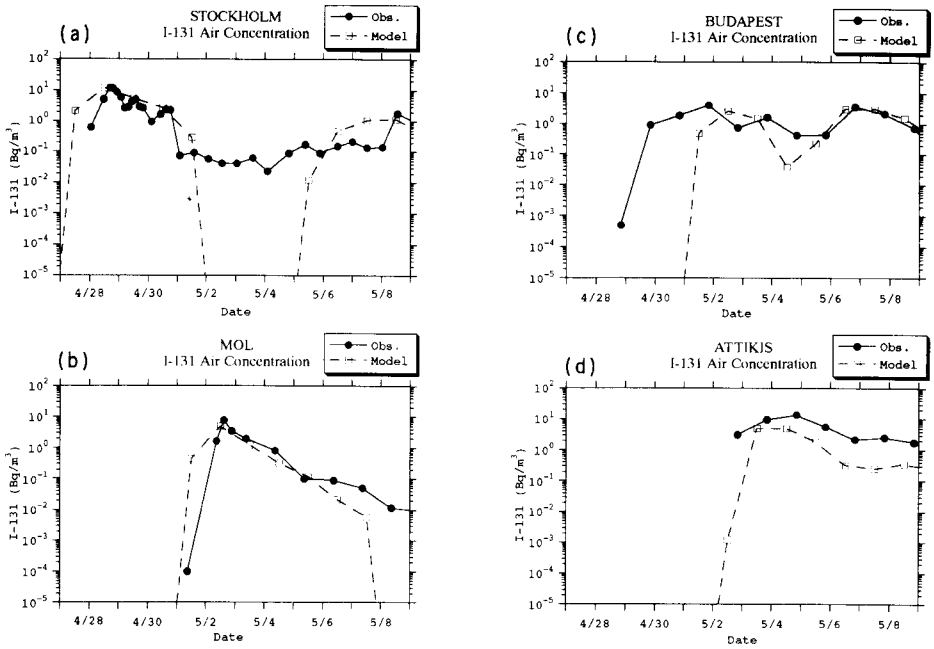

Fig.5. Air concentration of Cs- 137 at (a) Stockholm, Sweden ; (b) Mol, Belgium ; (c) Budapest, Hungary ; (d) Attikis, Greece. Solid line is the observation and dashed line is the model result.

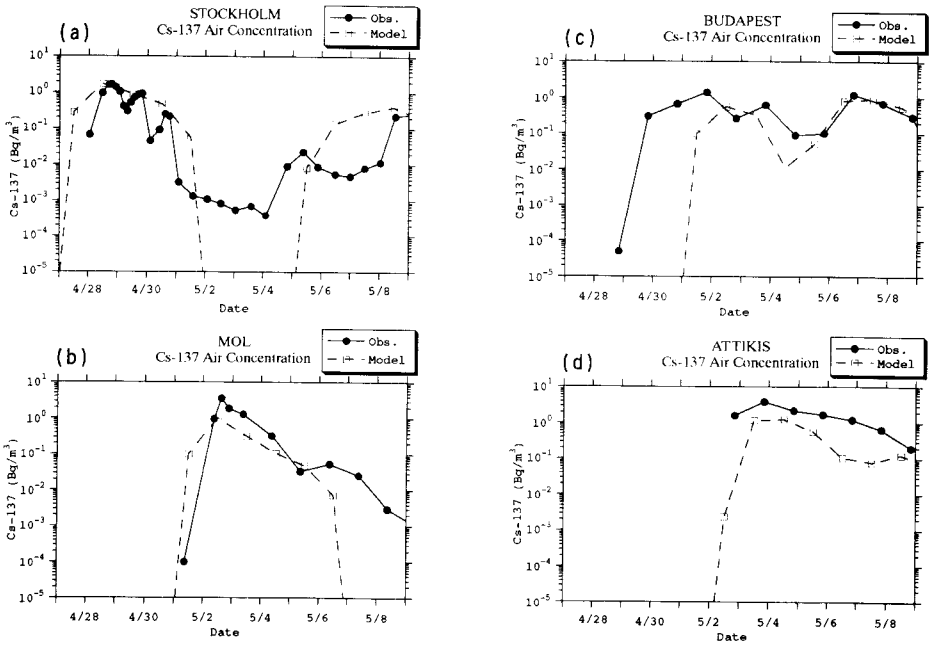

Fig.6. Same as Fig. 5, except for I-131 air concentration.

not discussed in detail for the following reasons:the significance of source-term specification would be lost by broadening the initial source width, and the discrepancy found at Stockholm would not be improved by the increase of the released particle number as realized in Fig. 4c.

3.3. Comparison with observations of deposition

Simulated and observed daily depositions of Cs-137 at Bilthoven and at Berlin are shown in Fig. 7a and b, respectively. The simulated deposition does not correspond well with the observation, although our model simulated well the air concentration at these two points as shown in Fig. 7c and d. This discrepancy is probably induced by the following two factors : the poor precipitation prediction in the model and the difference in the horizontal scale between observation and the model. The daily precipitation at Bilthoven and Berlin predicted by the model showed little correlation with the observation as shown in Fig. 8. Because most deposition of Cs-137 occurred in wet process (Hass *et al.*, 1990 ; Puhakka *et al.*, 1990), this poor prediction of the precipitation is undoubtedly one cause of the poor prediction of the deposition. On the other hand, the amount of wet deposition of the radioactive pollutants strongly depends on the place as well as precipitation : models must simulate the right position of location and time of precipitation and pollutants' arrival to predict the wet deposition accurately. If the precipitation and the wet deposition have a rather small scale, good prediction of wet deposition by the mesoscale model with $\delta x \approx 100$ km becomes difficult even in the case where the model predicts averaged precipitation well. In this sense, observed values do not represent wet deposition in the area with the horizontal scale of model 2 grid lengths ($\sim$ 250 km).

To improve the precipitation forecast, a new long-range transport model which uses a new routine weather forecasting model of the JMA as the weather forecasting part is being developed. In this model, both the horizontal and the vertical resolutions are improved to simulate fine-scale phenomena.

4. Summary

As a case study, we simulated the movements and deposition of radioactive pollutants released by the Chernobyl accident. The model was composed of the weather forecasting part that was the routine regional weather forecasting model of the JMA and the Lagrangian advection-diffusion part. The source data distributed by the ATMES project was used. In spite of there being no horizontal diffusion in our diffusion part, the simulated surface air concentration of Cs-137 and I-131 showed good correspondence with the observation. The effects of subgrid-scale horizontal diffusion were examined by extra simulations and it was found that the results were improved at some points but deteriorated at the other points.

Simulated deposition had poor correlation with the observed deposition. We consider poor precipitation forecast and the locality of observation are responsible for this discrepancy.

References

Air and Energy Engineering Research Lab., 1989: *The 1985 NAPAP emissions inventory (Version 2): Development of the annual data and modelers' tapes*, Environment Protection Agency, Research Triangle Park, pp. 2-2~2-3.

Alexander, R. C. and R. L. Mobley, 1976: Monthly average sea-surface temperature and ice-pack limits on a 1° global grid, *Mon. Wea. Rev.*, **104**, 143-104.

Arakawa, A. and V. R. Lamb, 1977 : Computational design of the basic dynamical process of the UCLA general circulation model, *Methods in Computational Physics*, **17**, 173-265.

Clark, M. J. and F. B. Smith, 1988 : Wet and dry deposition of Chernobyl releases, *Nature*, **332**, 245-249.

Eliassen, A., 1980 : A review of long-range transport modeling, *J. Appl. Meteor.*, **19**, 231-240.

Hass, H., M. Memmesheimer, H. Geiβ, H. J. Jakobs, M. Laube and A. Ebel, 1990 : Simulation of the Chernobyl radioactive cloud over Europe using the

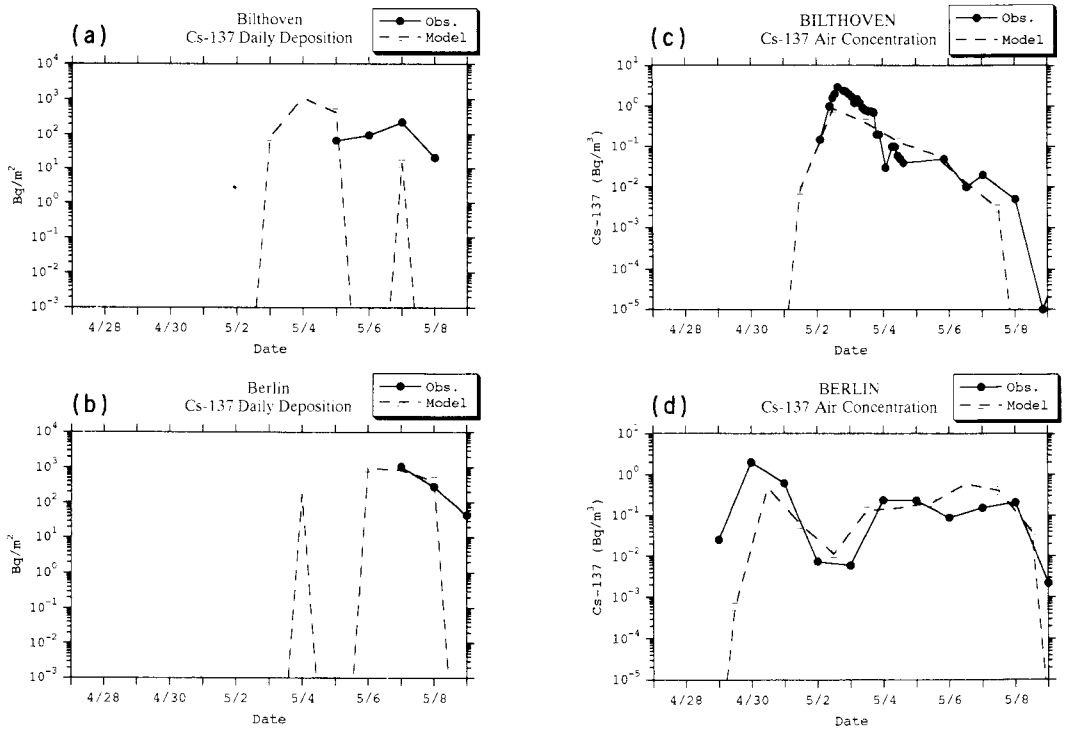

Fig.7. Daily deposition of Cs-137 at (a) Bilthoven, Netherlands, (b) Berlin, Germany, air concentration of Cs-137 at (c) Bilthoven and (d) Berlin. Solid line is the observation and dashed line is the model result.

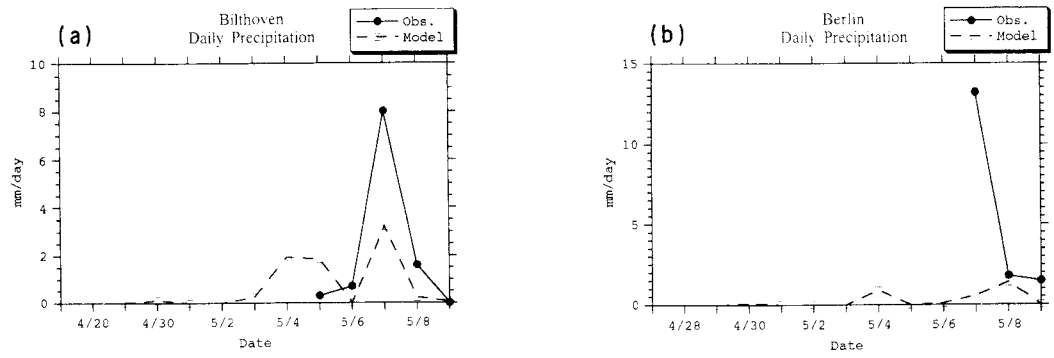

Fig.8. Daily precipitation at (a) Bilthoven and (b) Berlin.
Solid line is the observation and dashed line is the model result.

EURAD model, *Atmos. Env.*, **24A**, 673-692.

Johnson, W. B., 1983: Interregional exchanges of air pollution: Model types and applications, *J. Air Pollut. Control Assoc.*, **33**, 563-574.

Kimura, F. and T. Yoshikawa, 1988: Numerical simulation of global scale dispersion of radioactive pollutants from the accident at the Chernobyl nuclear power plant, *J. Meteor. Soc. Japan*, **66**, 489-495.

Klug, W., G. Graziani, G. Grippa, D. Pierce and C. Tassone, 1991a: *Atmospheric long-range transport model evaluation study*, Ispra.

Klug, W., G. Graziani, G. Grippa, D. Pierce and C. Tassone, 1991b: *Atmospheric long-range transport model evaluation study, Appendix volume*, Ispra.

Mellor, G. L. and T. Yamada, 1974: A hierarchy of turbulence closure models for planetary boundary layers, *J. Atmos. Sci.*, **31**, 1791-1807.

Numerical Prediction Division, 1986: *Outline of Operational Numerical Weather Prediction at Japan Meteorological Agency*, Japan Meteorological Agency, Tokyo, 93 p.

Pudykiewicz, J., 1990: A predictive atmospheric tracer model, *J. Meteor. Soc. Japan*, **68**, 213-225.

Puhakka, T., K. Jylhä P. Saarikivi and J. Koistinen, 1990: Meteorological factors influencing the radioactive deposition in Finland after the Chernobyl accident, *J. Appl. Meteor.*, **29**, 813-829.

Raes, F., G. Graziani, D. Stanners and F. Girardi, 1990: Radioactivity measurements in air over Europe after the Chernobyl accident, *Atmos. Env.*, **24A**, 909-916.

Raes, F., G. Graziani, L. Grossi, L. Marciano, D. Peirs, B. Pedersen, D. Stanners and N. Zarimpas, 1989: *Radioactivity measurements in Europe after the Chernobyl accident Part I: Air*, Commision of the European Communities, EUR 12269 EN, Ispra, 247 p.

Tatsumi, Y., 1983: An economical explicit time integration scheme for primitive model, *J. Meteor. Soc. Japan*, **61**, 269-288.

チェルノブイリ原子力発電所事故による放射性汚染物質の長距離拡散の数値シミュレーション

里村雄彦・木村富士男*・佐々木秀孝・吉川友章・村治能孝**

チェルノブイリ原子力発電所事故の際に放出された放射性汚染物質の，ヨーロッパにおける空気中濃度と沈着量について，気象研究所の長距離輸送モデルを用いて計算した。このモデルは，気象庁の現業ルーチンモデルで気象要素の予報を行い，ラグランジュ移流拡散モデルで汚染物質の濃度を計算する。発電所からの汚染物質の放出量として，ATMESプロジェクトで配布された発生源データを用いた。

計算の結果，モデルのCs-137とI-131の空気中濃度は観測とよく合うことが示された。しかし，沈着量は観測と合わないこともわかった。気象予測モデルの降水予報の精度の悪さと，観測値とモデルとがそれぞれ代表するスケールの違いが，沈着量の差の原因と考えられる。

* 現所属：筑波大学地球科学系
** （株）国際気象海洋
現所属：（株）エナジシェアリング